

Determination of Fragrance Allergens by Ultraviolet Femtosecond Laser Ionization Mass Spectrometry

Shibuta, Shimpei

Department of Applied Chemistry, Graduate School of Engineering, Kyushu University

Imasaka, Tomoko

Laboratory of Chemistry, Graduate School of Design, Kyushu University

Imasaka, Totaro

Division of International Strategy, Center of Future Chemistry, Kyushu University

<https://hdl.handle.net/2324/7165071>

出版情報 : Analytical chemistry. 88 (21), pp.10693-10700, 2016-11-01. American Chemical Society
バージョン :
権利関係 :



Determination of Fragrance Allergens by Ultraviolet Femtosecond Laser Ionization Mass Spectrometry

Shimpei Shibuta,[†] * Tomoko Imasaka,[§] and Totaro Imasaka[#]

[†]Department of Applied Chemistry, Graduate School of Engineering, Kyushu University, 744 Motoooka, Nishi-ku, Fukuoka 819-0395, Japan

[§]Laboratory of Chemistry, Graduate School of Design, Kyushu University, 4-9-1, Shiobaru, Minami-ku, Fukuoka 815-8540, Japan

[#]Division of International Strategy, Center of Future Chemistry, Kyushu University, 744 Motoooka, Nishi-ku, Fukuoka 819-0395, Japan

* To whom correspondence should be addressed. E-mail: shibuta.shimpei.238@s.kyushu-u.ac.jp

ABSTRACT

The allergenic compounds listed in the Cosmetics Directive by the Scientific Committee for Consumer Safety were analyzed by gas chromatography combined with multiphoton ionization mass spectrometry using a femtosecond laser emitting at 200 and 267 nm as the ionization source. The limits of detection were less than 100 pg/ μ L for all of the compounds, permitting them to be measured in actual samples that were simply prepared by a 100-fold dilution of the original sample. The ionization process was investigated for the 26 allergens, some of which had no absorption band, even in the far-ultraviolet region. As a result, non-resonant two-photon ionization was found to be the most sensitive and universal method for the trace analysis of these compounds, because of the short pulse width, i.e., a high peak power, of the femtosecond laser used. It should be noted that the excess energy can be reduced by using a laser emitting at longer wavelengths (267 nm), and that fragmentation can be suppressed, especially for a molecule that contains a long side chain. Three commercially available perfumes were measured, and more than 10 allergenic compounds were determined. Some of them were present at concentrations higher than the value specified in the Cosmetics Directive.

Quality of life is strongly affected by odors. Therefore, fragrances are frequently added to toiletries, cosmetics, and a variety of consumer products such as soap and food. In Japan, perfume is classified in the category of cosmetics and is controlled by a law, “the Drugs, Cosmetics and Medical Instruments Act”, which is equivalent to the corresponding laws in the other countries. In order to evaluate the safety of the fragrance ingredients, an organization entitled the “Research Institute for Fragrance Materials (RIFM)” was established in 1966, and major companies that produce fragrances have joined this organization. From the data provided by RIFM, the “International Fragrance Association (IFRA)” has determined various standards for their use. To date, almost all countries in the world follow the “IFRA Standard” for safety assurance. In Europe, where many cosmetics are produced and widely used, an organization entitled the “Scientific Committee for Consumer Safety (SCCS)” has published a “Cosmetics Directive” for companies that manufacture consumer products containing a variety of fragrances. In this document, 26 ingredients in such fragrances are specified as allergenic substances that should be listed on the label of the container when the concentrations are higher than 0.001% for leave-on products and 0.01% for rinse-off products.¹ These compounds are deemed to be hazardous in subjects who have been diagnosed with atopic dermatitis and asthma, allergic rhinitis and certain types of cancer.²⁻⁴ A positive patch test reaction to at least one of the 26 fragrance ingredients was identified in 115 (7.6%) of the subjects patch tested.⁵ Regulations in several countries and health and environmental concerns of fragrance products are summarized in the literature.⁶

The ingredients in a fragrance have been successfully measured by gas chromatography combined with olfactometry (GC/O) based on human perceptions.⁷ These compounds are more practically measured using GC combined with mass spectrometry (GC/MS). A variety of pretreatment techniques including headspace sampling and solid-phase microextraction (SPME) are

currently in use.⁸⁻¹¹ Advanced techniques based on two-dimensional gas chromatography (GC×GC) and tandem MS (MS-MS) have been utilized for samples that contain a larger number of allergens in complex matrices.^{12,13} Liquid chromatography combined with mass spectrometry (LC/MS) has also been employed for this purpose.¹⁴ Electron ionization (EI) is the most frequently used technique in MS for the measurement of allergens in a fragrance. This technique has been successfully used, since standard MS data are available for many of the organic compounds in databases and the analyte can be readily assigned. However, it is sometimes difficult to selectively determine the constituents because numerous interfering species are present in the sample. Therefore, a different ionization technique that would provide a molecular ion would be highly desirable for the comprehensive analysis of analytes contained in complex matrices.

Photoionization has been utilized for soft ionization, and provides a molecular ion in most cases.¹⁵ This technique is useful for the selective ionization of an analyte by optimizing the wavelength of the light source. In multiphoton ionization (MPI), the ionization efficiency can be improved using a laser with a pulse width shorter than the lifetime of the excited state. In addition, this technique can be used to reduce fragmentation.^{16,17} For example, polycyclic aromatic hydrocarbons (PAHs),¹⁸ dioxins (DXNs),¹⁸ and polychlorinated biphenyls (PCBs)¹⁹ can be selectively measured at ultratrace levels using ultraviolet (UV) femtosecond-ionization MS combined with GC. Since many organic compounds have absorption bands in the UV region and have lifetimes longer than the femtosecond time scale, this UV femtosecond ionization technique can be used to advantage for resonance-enhanced MPI (REMPI). However, numerous organic compounds have no absorption bands, even in the UV region. In this case, the analyte molecule must be ionized through a non-resonant MPI process. It should be noted that triacetone triperoxide (TATP), an explosive compound, has been efficiently ionized through a process of non-resonant

two-photon ionization (TPI) and it was possible to detect a molecular ion as the major ion by decreasing the excess energy in TPI and by decreasing the pulse width, even in the femtosecond region.²⁰ On the other hand, trinitrotoluene (TNT), another explosive compound, can be efficiently ionized through a process of resonant TPI, which produces a large molecular ion signal.²⁰ It should be noted that resonant TPI is more efficient than non-resonant TPI. However, the ratio of their efficiencies is reported to be only 1.2 at shorter pulse widths (75-90 fs) and 5.3 at longer pulse widths (600-700 fs) for 1-chloronaphthalene, although this value would depend on the molecule being examined.²¹ Allergenic substances in a fragrance can contain many types of compounds, as shown in Fig. S-1, i.e., aromatic/aliphatic hydrocarbons with/without conjugated/non-conjugated double bonds and short/long side chains. Because of this structural diversity, the 26 allergenic compounds in a fragrance would be a sufficiently complex mixture of organic compounds for evaluating the advantages of using UV femtosecond ionization in MS.

In this study, we measured 26 allergenic compounds by GC/MPI-MS using a femtosecond laser emitting at 200 and 267 nm as the ionization source. The limits of detection (LODs) were determined and compared to each other to evaluate the advantage of this method based on resonant/non-resonant TPI using spectral data obtained by quantum chemical calculations. This analytical technique was applied to the comprehensive analysis of the allergenic compounds in three types of perfumes after they were subjected to a 100-fold dilution.

EXPERIMENTAL SECTION

Analytical Instrumentation. The analytical instrument used in this study has been described elsewhere in detail and is briefly described in this section.¹⁷ As shown in Fig. S-2, a GC (6890N,

Agilent Technologies, Santa Clara, CA, USA) was combined with a time-of-flight mass spectrometer (TOFMS) developed in this laboratory and is now commercially available (HK-1, Hikari-GK, Fukuoka, Japan). The third harmonic (267 nm, 16 or 130 μ J) and fourth harmonic (200 nm, 16 μ J) emissions of a Ti:sapphire laser (800 nm, 35 fs, 4 mJ, 1 kHz, Elite, Coherent, Santa Clara, CA, USA) was used as the ionization source in MS.¹⁷ A DB-5ms column (30 m long, 0.25 mm i.d., 0.25 mm film thickness, Agilent Technologies) was utilized for separating the 26 allergenic compounds. The temperature of the GC oven was set at 45 °C and held for 2 min, and was then programmed to increase at a rate of 8 °C/min to 100 °C and again to 150 °C at a rate of 20 °C/min. The temperature was further increased to 200 °C at a rate of 25 °C/min, with a 5 min hold and then to 233 °C at a rate of 8 °C/min. The flow rate of helium used as a carrier gas was 1 mL/min. A transfer line connecting the GC and the MS was maintained at 200 °C. The analytes eluting from the capillary column were introduced into the MS and the laser beam was focused on the analyte that was entrained in a molecular beam. The induced ions were accelerated into a TOF tube and were measured using an assembly of microchannel plates (F4655-11, Hamamatsu Photonics, Shizuoka, Japan). The signals recorded by a digitizer (AP240, Agilent Technology) were analyzed using the software programmed by LabVIEW and ORIGIN.

Sample. The 26 allergenic substances shown in Fig. S-1 were purchased from Wako Pure Chemical Industries, Tokyo, Japan (1, pinene; 2, limonene; 3, benzyl alcohol; 4, linalool, 5, methyl-2-octynoate; 6, citronellol; 7, citral; 8, geraniol; 9, cinnamaldehyde; 10, hydroxycitronellal; 11, anis alcohol; 12, cinnamyl alcohol; 13, eugenol; 14, methyl eugenol; 15, isoeugenol; 16, coumarin; 17, ionone; 18, linal; 19, amylcinnamaldehyde; 20, lylal; 21, amyl cinnamic alcohol; 22, farnesol; 23, hexylcinnamaldehyde; 24, benzyl benzoate; 26, benzyl cinnamate: the analytes are

numbered according to the order of their elution in GC) and from Tokyo Chemical Industry, Tokyo, Japan (25, benzyl salicylate). Three types of perfumes, i.e., Sakura Eau de Toilette (the names of the ingredients listed on the label of the container were as follows: Alcohol Denat. 66%, Aqua, Parfum, Hexyl Cinnamal. PEG-40 Hydrogenated Caster Oil, Trideceth-9, Linalool, Alpha-Isomethyl Ionone, Butylphenyl Methylpropional, Hydroxyisohexyl 3-Cyclohexene Carboxaldehyde, Propylene Glycol, Citronellol, Hydroxycitronellal, *t*-Butyl Alcohol, Limonene, Helianthus Annuus Seed Oil, Geraniol, Prunus Serrulata Flower Extract, Benzyl Benzoate, Citral, Denatunium Benzoate), Moroccan Rose (Alcohol Denat. 66.9%, Aqua, Parfum, Geraniol, Limonene, Citronellol, Hydroxycitronellal, *t*-Butyl Alcohol, Linalool, Rosa Centifolia Flower Oil, Denatonium Benzoate, Alpha-Isomethyl Ionone, Citral, Eugenol), and White Musk (no list was attached), were purchased from a local souvenir shop. Individual stock solutions of the standards were prepared in methanol and were further diluted with acetone.¹⁴ The perfumes were diluted 100 fold with acetone and were measured without any other pretreatment procedures.

Quantum Chemical Calculation. The spectral properties of the 26 allergens were evaluated based on quantum chemical calculations to investigate the ionization mechanism. The optimized geometry of the ground state and harmonic frequencies were calculated using the ω B97XD method²² based on density functional theory (DFT) with a cc-pVDZ basis set²³. A vertical ionization energy (*IE*) was calculated from the difference between the energies of the ground and ionic states at the level of ω B97XD/c-pVDZ. The lowest 40 singlet transition energies and the oscillator strengths were calculated using time-dependent DFT (TD-DFT)²⁴. The predicted absorption spectra were obtained by assuming a Gaussian profile with a half width at half maximum of 0.333 eV. The calculations were performed using the Gaussian 09²⁵ and Gauss View 5²⁶ software programs.

RESULTS AND DISCUSSION

1. STANDARD SAMPLES

1.1 Two-dimensional Display. A standard sample mixture containing the 26 allergens, each of which was prepared at a concentration of 200 pg/ μ L, was measured by GC/MPI-TOFMS using a far-UV femtosecond laser (200 nm, 16 μ J). Numerous spots were observed on the two-dimensional display of the GC/MS, i.e., the retention time in GC vs. the mass/charge ratio (m/z) in MS. As shown in Table S-1, not all of the 26 allergen molecules were always detected (see the molecules denoted as n.d. in the table). The sample was then measured using a deep-UV femtosecond laser (267 nm, 16 μ J), although many of these compounds had no absorption band at this wavelength. Contrary to our expectations, all of the 26 allergy molecules were detected, although some should have been ionized through a process of non-resonant TPI. In order to enhance the signal intensity, the sample was measured at a larger pulse energy produced by the third harmonic generation (130 μ J). The LODs for the compounds measured are summarized in Table S-1. The values shown in the last column (267 nm, 130 μ J) were less than 100 pg/ μ L, suggesting that this instrument has sufficient sensitivity to permit the 26 allergens ($0.001\% \approx 10$ ng/ μ L for leave-on sample) specified in the Cosmetic Directive to be measured, even after a 100-fold dilution.

1.2 Ionization Mechanism. It is well known that resonant TPI is more efficient than non-resonant TPI. We therefore expected a more efficient ionization and, as a result, lower LODs when measured at 200 nm rather than at 267 nm, since a laser emitting in the far-UV region is more useful for resonant TPI. As shown in Table S-1, the LOD values were dependent on the allergenic compounds measured, and the values obtained at 130 μ J were not measurably better (sometimes even poorer) than those obtained at 16 μ J (267 nm). Therefore, the ionization mechanism for

achieving efficient ionization and for obtaining a molecular ion against the 26 allergenic compounds was examined and is discussed in the following sections.

1.2.1 Resonant Ionization Both at 200 and 267 nm.

Cinnamaldehyde. Figure 1 shows the absorption spectrum calculated by TD-DFT and the mass spectra measured at 200 and 267 nm and 16 and 130 μJ for cinnamaldehyde (see the figure caption for details). The calculated absorption spectrum suggests the occurrence of efficient resonant TPI at wavelengths of both 200 and 267 nm. In fact, a large molecular ion signal, in addition to a few fragment ions, was observed at 200 nm and 16 μJ as shown in Fig. 1 (B). However, fragmentation was more pronounced when measured at 267 nm as shown in Fig. 1 (C), which is probably due to photo fragmentation by efficiently absorbing a few photons because of the large molar absorptivity at 267 nm. Thus, the signal intensity of the molecular ion was decreased, even though the molar absorptivity at 267 nm was larger than that at 200 nm. The signal intensity can be increased at a larger pulse energy (130 μJ) as shown in Fig. 1 (D). However, the fragmentation appears to be more pronounced. As a result, the value for the LOD obtained using the molecular ion was the lowest (0.24 $\text{pg}/\mu\text{L}$) at 200 nm (16 μJ) and increased to 0.85 $\text{pg}/\mu\text{L}$ (16 μJ) and 0.89 pg/mL (130 μJ) at 267 nm. It is interesting to note that the signals measured at 267 nm and 130 μJ appear to be broadened. This unfavorable result can be attributed to a space charge effect: a large number of ions are formed in the ionization region and are scattered from each other to increase the initial velocity distribution. Note that a linear-type TOFMS used in this study does not compensate for the initial velocity distribution and provides information concerning the kinetic energy of the ions in MS. This effect, i.e., peak broadening, could be reduced by diluting the sample or by defocusing the laser beam to expand the ionization region.

The spectral properties of isoeugenol are similar to those for cinnamaldehyde as shown in Fig.

S-3, providing LODs of 0.19, 0.63, and 0.44 pg/ μ L at 200 nm (16 μ J), 267 nm (16, 130 μ J), respectively. The situation is similar to benzyl salicylate as shown in Fig. S-4: LODs were 2.1, 2.0, and 1.1 pg/ μ L, respectively. This group of compounds have absorption bands both at 200 and 267 nm and can be easily determined by UV femtosecond-ionization MS.

Hexylcinnamaldehyde. The calculated absorption spectrum shown in Fig. 2 (A) suggests resonant TPI at wavelengths of both 200 and 267 nm. This result is similar to cinnamaldehyde. The LOD value obtained at 200 nm (16 μ J) was 5.3 pg/ μ L, which was improved to 1.2 pg/ μ L by changing the laser wavelength to 267 nm, as is shown in Table S-1. This improvement in LOD can be attributed to a larger molar absorptivity and/or a smaller excess energy for ionization at 267 nm (0.80 eV) than at 200 nm (3.92 eV). In fact, the fragmentation is slightly more extensive when measured at 200 nm (Fig. 2 (B)), compared with the data measured at 267 nm (Fig. 2 (C)). In addition, the fragment peaks shown in Fig. 2 (B) are broader than the molecular ion peak, suggesting a larger velocity distribution for the fragment ions by the large excess energy at 200 nm. As shown in Fig. 2 (D), the signal intensity increased with increasing laser pulse energy (130 μ J), providing a lower LOD (0.59 pg/ μ L). However, the signal intensity is not in proportional to the laser pulse energy, suggesting that the signal was saturated, e.g., by photo dissociation or a lack of remaining molecules in the ionization region.

Amylcinnamaldehyde has similar spectral properties as shown in Fig. S-5: the LODs were 36, 1.55, 0.76 pg/ μ L at 200 nm (16 μ J) and 267 nm (16, 130 μ J), respectively: photo decomposition was more serious at 200 nm for this compound. Accordingly, the excess energy (3.29 eV at 200 nm) should be minimal for the measurement of a molecule with a long side chain. Benzyl cinnamate can be also categorized as a member of this group (see Fig. S-6), since this compound has a long chain at the center part of a molecule and has a large excess energy (3.93 eV) at 200 nm. As a result,

efficient photo dissociation would occur, providing rather poor LODs (n.d., 110, 10 pg/ μ L).

Coumarin. The calculated absorption spectrum for coumarin shown in Fig. 3 (A) suggests resonant TPI at both 200 and 267 nm, and the excess energy is minimal at 267 nm and is also small, even at 200 nm. Moreover, this compound contains no side chain, suggesting very efficient ionization both at 200 and 267 nm. On the other hand, it is well known that coumarin is a strongly fluorescent compound, suggesting a long excited-state lifetime. For these reasons, we expected that this compound would be efficiently ionized and would provide a large signal for a molecular ion even when a nanosecond laser were used as the ionization source. However, the signal intensities measured at 200 and 267 nm were quite small, as shown in Figs. 3 (B) and (C), even when a UV femtosecond ionization was employed. In fact, the LOD values were 16 and 9.7 pg/ μ L at 200 and 267 nm (16 μ J), respectively. At a larger pulse energy (130 μ J), the signal intensity was enhanced but the fragmentation was also more pronounced, leading to a rather poor LOD (5.1 pg/ μ L). The mechanism responsible for this unfavorable result remains unclear at this time. A possible explanation would be efficient photo decomposition of the molecule to a neutral species, but further studies would be necessary for obtaining a better understanding of this curious compound.

1.2.2 Resonant Ionization at 200 nm and Non-resonant Ionization at 267 nm.

Eugenol. The calculated absorption spectrum of eugenol is shown in Fig. 4 (A), suggesting resonant TPI at 200 nm and non-resonant or nearly-resonant TPI at 267 nm. However, there were no major differences in the data measured at the same pulse energy (16 μ J) at 200 and 267 nm as shown in Figs. 4 (B) and (C). When the pulse energy was increased to 130 μ J at 267 nm, the fragment ions appeared to be more pronounced and the signal peaks were broadened, as shown in Fig. 4 (D). This undesirable effect would arise from the space charge effect described in the previous section. The LOD was 0.20, 0.70, and 0.60 pg/ μ L at 200 nm (16 μ J), 267 nm (16, 130 μ J),

respectively. These results suggest that this type of molecule can be efficiently ionized, even under the near-resonant (or non-resonant) conditions. It should be noted that a molecular ion can be observed, even at a large excess energy (4.81 eV at 200 nm). This suggests that fragmentation can be reduced for aromatic molecules with short side chains.

The spectral properties of methyl eugenol are similar to those for eugenol as shown in Fig. S-7, providing similar LODs of 0.26, 0.63, and 0.66 pg/ μ L at 200 nm (16 μ J), 267 nm (16, 130 μ J), respectively. The situation would be similar to the behavior of other aromatic compounds such as anis alcohol (Fig. S-8; 0.82, 0.60, 0.25 pg/ μ L), benzyl benzoate (Fig. S-9; 2.3, 3.2, 1.6 pg/ μ L), and lilial (Fig. S-10; 2.8, 0.59, and 0.48 pg/ μ L). Ionone, a non-aromatic molecule that contains an aliphatic ring with double bonds (Fig. S-11; 0.99, 0.87, 0.82 pg/ μ L), and citral, an aliphatic molecule with double bonds (Fig. S-12; 40, 2.8, 2.4 pg/ μ L), would also be involved in this category. As expected, the effect of resonance is appreciable, but not so significant. An aromatic molecule can be measured with better sensitivity than a molecule containing a non-aromatic ring, which can be measured with better sensitivity than an aliphatic molecule, due to their more stable structure.

Amyl cinnamic alcohol. From Fig. 5 (A), this aromatic molecule would be expected to be ionized through a process of resonant TPI at 200 nm and through non-resonant or near-resonant TPI at 267 nm as in the case of eugenol. However, no signal was observed at 200 nm, as shown in Fig. 5 (B). On the other hand, a large signal for a molecular ion was observed at 267 nm (Fig. 5 (C)), which was further enhanced when a larger pulse energy (130 μ J) was used with slightly enhanced fragmentation (Fig. 5 (D)), providing LODs of 1.6 and 2.8 pg/ μ L at 267 nm (16, 130 μ J). This result can be explained by a large excess energy (4.41 eV) at 200 nm and photo decomposition due to a long side chain in a molecule. This situation would be similar to cinnamyl alcohol (Fig. S-13; 24, 5.4, 0.58 pg/ μ L).

Benzyl alcohol. This compound can be ionized through near-resonant TPI at 200 nm and non-resonant TPI at 267 nm, as shown in Fig. 6 (A). Due to the large excess energy at 200 nm (3.72 eV), a large fragment ion signal, $[M-1]^+$, was observed, as shown in Fig. 6 (B). Fragmentation was suppressed when measured at 267 nm, as shown in Fig. 6 (C). This favorable result can be attributed to the decrease in excess energy at 267 nm (0.60 eV). The signal intensity is further enhanced at a larger pulse energy of 130 μ J, as shown in Fig. 6 (D). These results suggest that a reduction in excess energy is important for suppressing fragmentation as well as for enhancing a molecular ion. The LOD was 0.72, 0.93, and 0.30 pg/ μ L at 200 nm (16 μ J) and 267 nm (16, 130 μ J), respectively, low LODs being achieved due to a short side chain in a molecule. As described before, the effect of resonance is minimal in UV femtosecond ionization and the LOD value can be improved at larger pulse energies.

Lyrar. As shown in Fig. 7 (A), this molecule, with a ring structure containing a double bond, would be non-resonantly or near-resonantly ionized at 200 nm and non-resonantly at 267 nm. Due to the large excess energy (3.87 eV) and the presence of a long aliphatic side chain, no signal was observed at 200 nm, as shown in Fig. 7 (B). On the other hand, a molecular ion, in addition to several fragment ions, was observed at 267 nm (16 μ J) as shown in Fig. 7 (C), and the signals were further enhanced at a larger pulse energy of 130 μ J. As a result, the LODs were n.d., 11, 2.1 pg/ μ L at 200 nm (16 μ J) and 267 nm (16, 130 μ J), respectively. Compared with benzyl alcohol, the signal intensity was smaller, probably due a smaller absorptivity and/or the non-aromatic nature of this molecule.

Pinene (Fig. S-14; 21, 2.2, 0.74 pg/ μ L) and limonene (Fig. S-15; 4.3, 1.7, 0.62 pg/ μ L) contain an aliphatic ring structure, and, as a result, these molecules can be grouped in this category. However, these molecules do not contain a long side chain, and can be detected with better sensitivity. Thus, a

non-aromatic ring molecule with short side chains can be efficiently ionized by non-resonant TPI using a UV femtosecond laser with a large pulse energy.

Methyl-2-octynoate, an aliphatic molecule with a triple bond, has a small absorption band at 200 nm and no absorption band at 267 nm, as shown in Fig. S-16, which is similar to lylal. The LODs were rather poor (51, 47, 6.4 pg/ μ L), probably due to the presence of a flexible long-chain structure, coupled with the more dissociative nature of this molecule.

1.2.3 Non-resonant Ionization at 200 and 267 nm.

Linalool. As shown in Fig. 8 (A), this molecule contains neither a ring structure nor a conjugated double bond, in contrast to lylal in the previous section. Accordingly, this molecule has no (or a very small) absorption band, even at the wavelength of 200 nm. As a result, it would be expected to be ionized through a non-resonant process both at 200 and 267 nm. Due to a large excess energy (3.97 eV) at 200 nm and a long aliphatic chain, the signal peak was very weak, as shown in Fig. 8 (B): the signal was not observed as a MS peak but was observable as a GC peak. A molecular ion was observed at 267 nm (16 μ J) and more distinctively at 130 μ J, as shown in Figs. 8 (C) and (D). Accordingly, the LOD was 106, 150, 19 pg/ μ L at 200 nm (16 μ J) and 267 nm (16, 130 μ J).

The other compounds in this category would be farnesol (S-17; 28, 34, 9.1 pg/ μ L), geraniol (Fig. S-18; 25, 10, 3.4 pg/ μ L), citronellol (Fig. S-19; 20, 9.9, 1.3 pg/ μ L), and hydroxycitronellal (Fig. S-20: 83, 37, 20 pg/ μ L). As demonstrated herein, this group of compounds is the most difficult to be measured using UV femtosecond-ionization MS.

2. ACTUAL SAMPLES

2.1 Two-dimensional Display. Three types of perfumes were analyzed using GC/MPI-TOFMS,

and two of them are shown in Fig. 9. More than 10 allergenic compounds are observed in the two-dimensional display. It should be noted that the signals arising from such allergenic compounds are clearly separated from the interfering species in the sample matrix, suggesting that the selectivity of GC/MPI-TOFMS is sufficient for a trace analysis of the ingredients in a perfume sample. Figure 10 shows an expanded view where eugenol, anis alcohol, and cinnamyl alcohol appear in the two-dimensional display. This picture indicates that eugenol is present only in the Sakura Eau de Toilette sample.

2.2 Ingredients in Fragrances. Figure S-21 shows the concentrations of allergens contained in the three perfumes. Their concentrations are very different from each other. It is apparent that the concentrations of methyl-2-octynoate, citronellol, hexylcinnamaldehyde, and linalool (not shown in Fig. S-21) in Sakura Eau de Toilette, and methyl-2-octynoate in White Musk are larger than the concentration specified by the Cosmetics Directive (0.001% for a leave-on sample).

CONCLUSIONS

A variety of allergenic substances in fragrances were measured using GC/MPI-TOFMS, and the effects of the laser wavelength (200 and 267 nm) and the pulse energy (16, 130 μ J) on ionization efficiency and LOD were investigated using spectral data obtained by quantum chemical calculations. The 26 allergenic compounds had very different spectral properties to each other and were useful for examining the potential advantage of this technique, based on UV femtosecond ionization. As a result, resonant TPI provided superior results in some cases. However, such a favorable effect was minimal in many cases. When the ionization energy was lower than two photon energy of the laser, the excess energy was increased (especially at 200 nm), which resulted in an accelerated fragmentation/decomposition, especially for a molecule with a flexible side chain:

a tunable UV femtosecond laser would be useful for minimizing the excess energy and to efficiently ionize a molecule through a non-resonant TPI process. For this reason, the lowest LODs were mostly obtained at 267 nm and 130 μ J using the third harmonic emission of the Ti:sapphire laser, LODs of <100 pg/ μ L being achieved for all the 26 allergenic compounds. The ingredients in the perfume were clearly resolved on the two-dimensional display, and their concentrations were determined after the sample was diluted by 100-fold.

ACKNOWLEDGMENTS

This research was supported by a Grant-in-Aid for Scientific Research from the Japan Society for the Promotion of Science (JSPS KAKENHI Grant Number 26220806, 15K13726, and 15K01227). The computation was mainly carried out using the computer facilities at Research Institute for Information Technology, Kyushu University.

REFERENCES

1. CNFP/0017/98 Final FRAGRANCE ALLERGY IN CONSUMERS (December 1999).
2. Mortz, C. G.; Lauritsen, J. M.; Bindslev-Jensen, C.; Andersen, K. E. *Br. J. Dermatol.* **2001**, *144*, 523-532.
3. Schlueter, D. P.; Soto R. J.; Baretta, E. D.; Herrmann, A. A.; Ostrander L. E.; Stewart R. D. *Chest* **1979**, *75*, 544-548.
4. Johnson, J. D.; Ryan, M. J.; Toft, J. D. II, Graves, S. W.; Hejtmancik, M. R.; Cunningham, M. L.; Herbert, R.; Abdo, K. M. *J. Agrec. Food Chem.* **2000**, *48*, 3620-3632.
5. Heisterberg, M. V.; Menné, T.; Johansen, J. D. *Contact Dermatitis* **2011**, *65*, 266-275.
6. Bridges, B. *Flavour Fragr. J.* **2002**, *17*, 361-371.
7. Bartsch, J.; Uhde, E.; Salthammer, T. *Anal. Chim. Acta* **2016**, *904*, 98-106.
8. Pablo Lamas, J.; Sanchez-Prado, L.; Garcia-Jares, C.; Llompart, M. *Anal. Bioanal. Chem.* **2009**, *394*, 1399-1411.
9. Becerril, E.; Lamas, J. P.; Sanchez-Prado, L.; Llompart, M.; Lores, M.; Garcia-Jares, C. *Talanta* **2010**, *83*, 464-474.
10. Rastogi, S. C. *J. High Resol. Chromatogr.* **1995**, *18*, 653-658.
11. Desmedt, B.; Canfyn, M.; Pype, M.; Baudewyns, S.; Hanot, V.; Courselle, P.; De Beer, J. O.; Rogiers, V.; De Paepe, K.; Deconinck, E. *Talanta* **2015**, *131*, 444-451.
12. Shellie, R.; Marriott, P.; Chaintreau, A. *Flavour Fragr. J.* **2004**, *19*, 91-98.
13. Lv, Q.; Zhang, Q.; Li, W.; Li, H.; Li, P.; Ma, Q.; Meng, X.; Qi, M.; Bai, H. *J. Sep. Sci.* **2013**, *36*, 3534-3549.
14. Famiglini, G.; Termopoli, V.; Palma, P.; Capriotti, F.; Cappiello, A. *Electrophoresis* **2014**, *35*, 1339-1345.

15. Boesl, U.; Zimmermann, R.; Weickhardt, C.; Lenoir, D.; Schramm, D. -W.; Kettrup, A.; Schlag, E. W. *Chemosphere* **1994**, *29*, 1429-1440.
16. Ledingham, K. W. D.; Singhal, R. P. *Int. J. Mass Spectrom.* **1997**, *163*, 149-168.
17. Imasaka, T. *Anal. Bioanal. Chem.* **2013**, *405*, 6907-6912.
18. Matsui, T.; Fukazawa, K.; Fujimoto, M.; Imasaka, T. *Anal. Sci.* **2012**, *28*, 445-450.
19. Matsui, T.; Uchimura, T.; Imasaka, T. *Anal. Chim. Acta* **2011**, *694*, 108-114.
20. Hamachi, A.; Okuno, T.; Imasaka, T.; Kida, Y.; Imasaka, T. *Anal. Chem.* **2015**, *87*, 3027-3031.
21. Kouno, H.; Imasaka, T. *Analyst*, DOI: 10.1039/c6an00577b.
22. Chai, J. D.; Head-Gordon, M. *Phys. Chem. Chem. Phys.* **2008**, *10*, 6615–6620.
23. Dunning Jr., T. H. *J. Chem. Phys.* **1989**, *90*, 1007-23.
24. Bauernschmitt, R.; Ahlrichs, R. *Chem. Phys. Lett.* **1996**, *256*, 454-64.
25. Gaussian 09, Revision E.01, Frisch, M. J. et al. *Gaussian, Inc.*, Wallingford CT, 2009.
26. GaussView, Version 5, Dennington, R.; Keith, T.; Millam, J. *Semichem Inc.*, Shawnee Mission, KS, 2009.

Figure Captions

- Fig. 1 (A) Calculated absorption spectrum for cinnamaldehyde. Mass spectra measured at (B) 200 nm, 16 μ J (C) 267 nm, 16 μ J (D) 267 nm, 130 μ J. *EE*, the lowest transition energy; *IE*, ionization energy; *IE/2*, a half of the ionization energy.
- Fig. 2 (A) Calculated absorption spectrum for hexylcinnamaldehyde. Mass spectra measured at (B) 200 nm, 16 μ J (C) 267 nm, 16 μ J (D) 267 nm, 130 μ J.
- Fig. 3 (A) Calculated absorption spectrum for coumarin. Mass spectra measured at (B) 200 nm, 16 μ J (C) 267 nm, 16 μ J (D) 267 nm, 130 μ J.
- Fig. 4 (A) Calculated absorption spectrum for eugenol. Mass spectra measured at (B) 200 nm, 16 μ J (C) 267 nm, 16 μ J (D) 267 nm, 130 μ J.
- Fig. 5 (A) Calculated absorption spectrum for amyl cinnamic alcohol. Mass spectra measured at (B) 200 nm, 16 μ J (C) 267 nm, 16 μ J (D) 267 nm, 130 μ J.
- Fig. 6 (A) Calculated absorption spectrum for benzyl alcohol. Mass spectra measured at (B) 200 nm, 16 μ J (C) 267 nm, 16 μ J (D) 267 nm, 130 μ J.
- Fig. 7 (A) Calculated absorption spectrum for lyral. Mass spectra measured at (B) 200 nm, 16 μ J (C) 267 nm, 16 μ J (D) 267 nm, 130 μ J.
- Fig. 8 (A) Calculated absorption spectrum for linalool. Mass spectra measured at (B) 200 nm, 16 μ J (C) 267 nm, 16 μ J (D) 267 nm, 130 μ J.
- Fig. 9 Two-dimensional display measured for the actual samples. (A) Sakura Eau de Toilette (B) Moroccan Rose. The sample was diluted 100 fold and measured using GC/MPI-TOFMS. Laser wavelength, 267 nm; laser pulse energy, 130 μ J.
- Fig. 10 Expanded views of the two-dimensional display shown in Fig. 9.

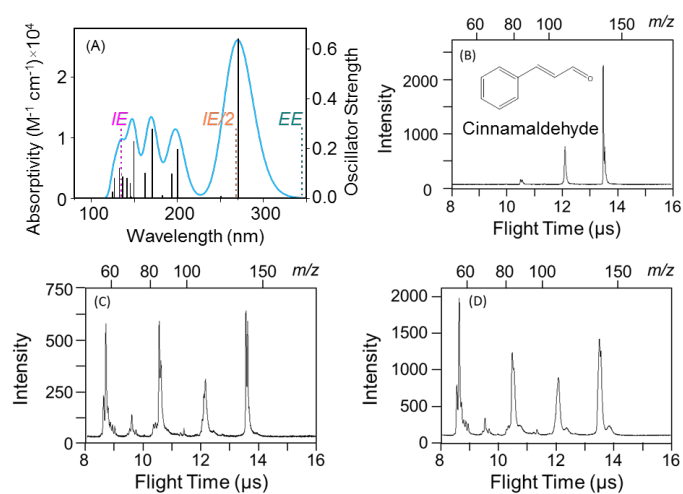


Fig. 1 S. Shibuta et al.

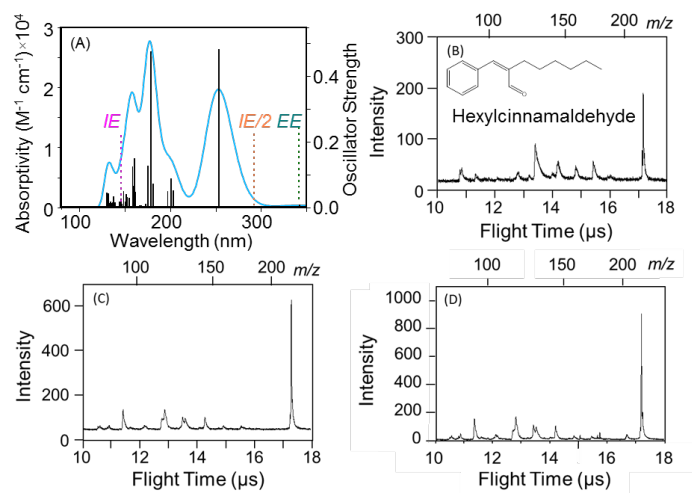


Fig. 2 S. Shibuta et al.

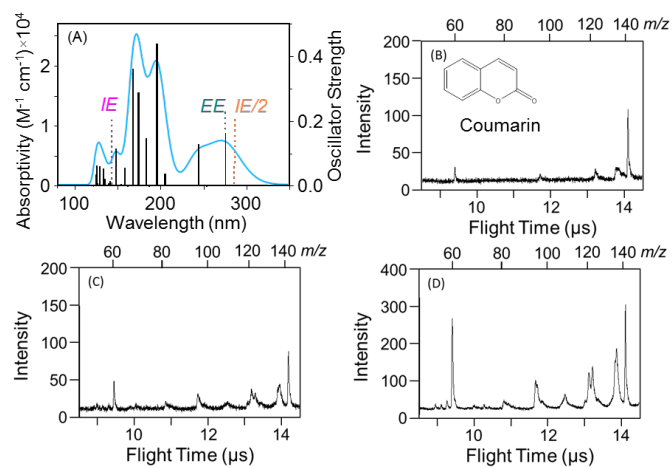


Fig. 3 S. Shibuta et al.

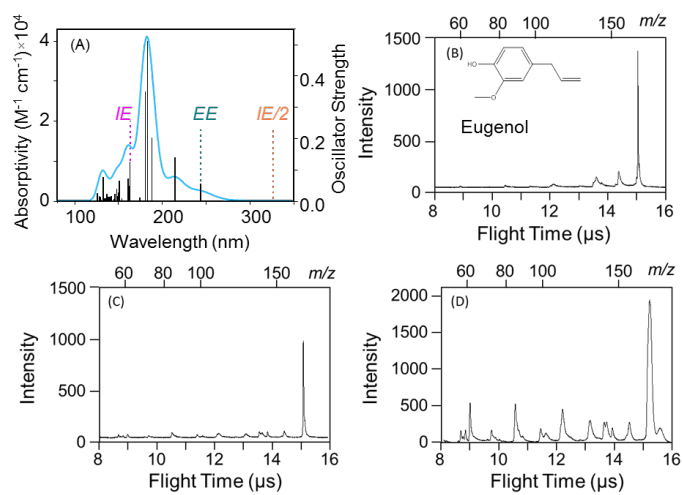


Fig. 4 S. Shibuta et al.

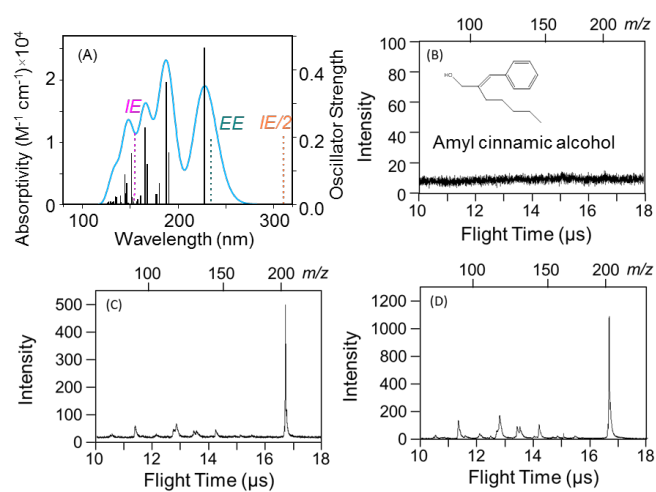


Fig. 5 S. Shibuta et al.

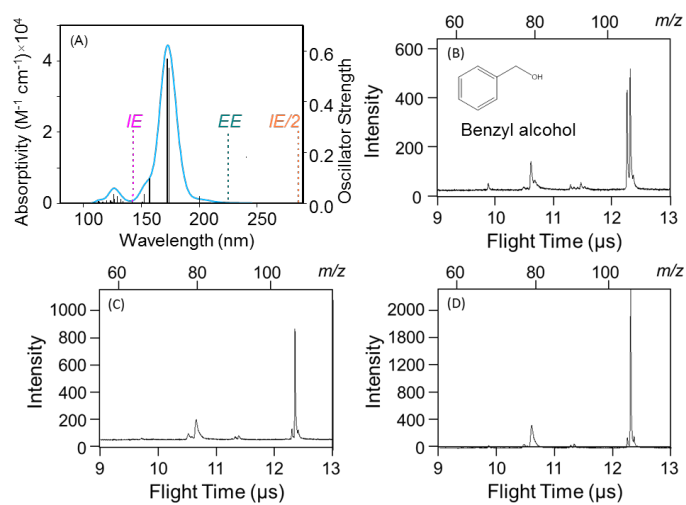


Fig. 6 S. Shibuta et al.

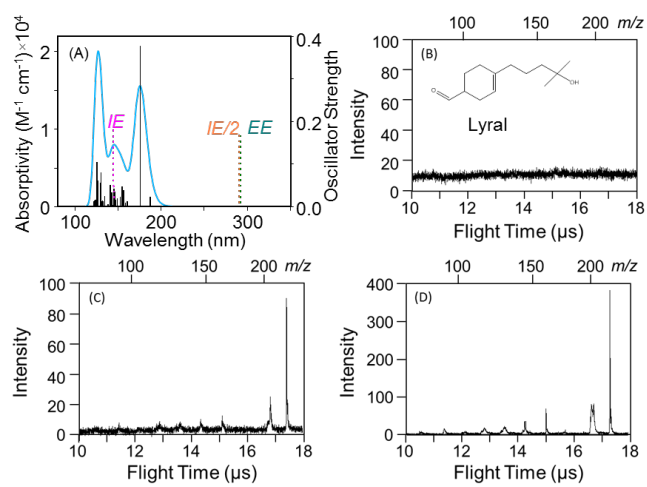


Fig. 7 S. Shibuta et al.

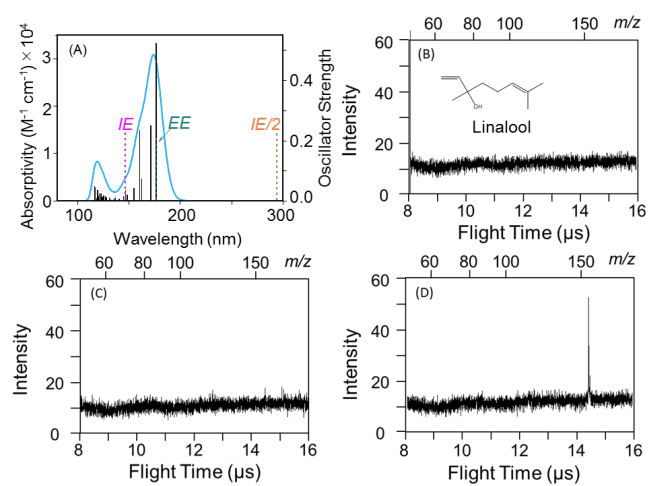


Fig. 8 S. Shibuta et al.

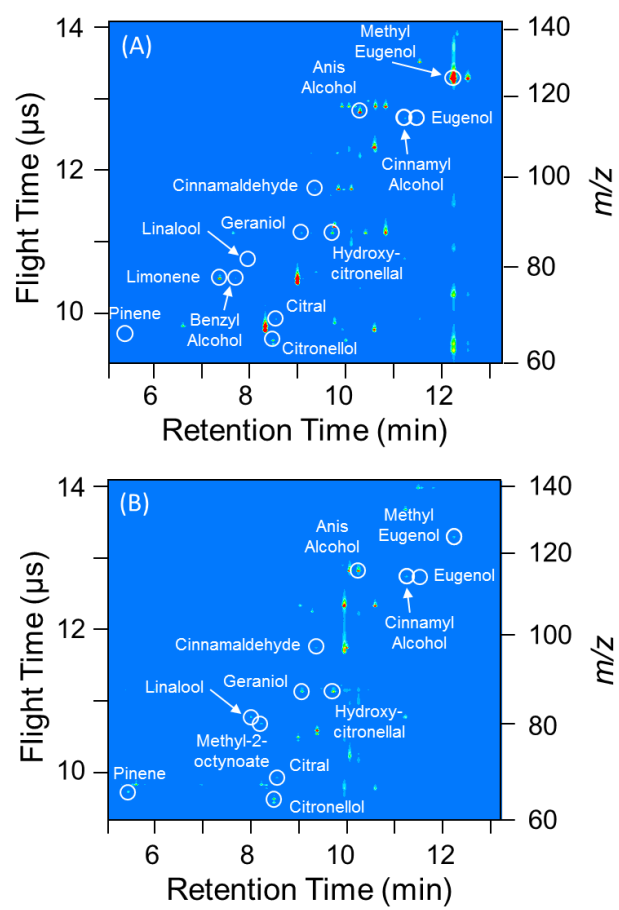


Fig. 9 S. Shibuta et al.

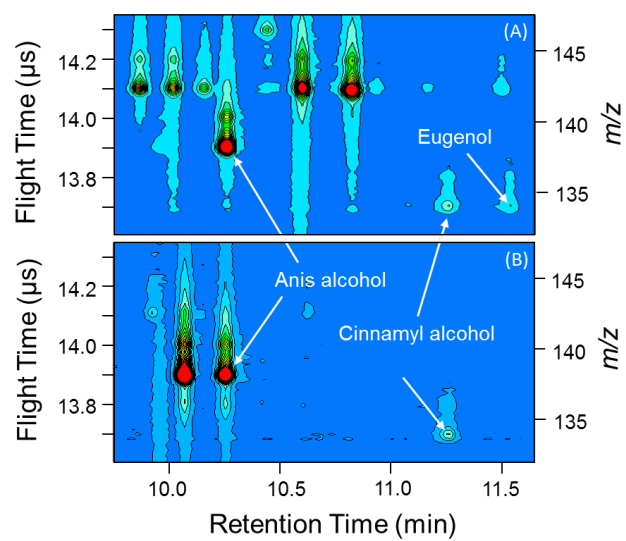


Fig. 10 S. Shibuta et al.